

Versatile synthesis and micropatterning of nonfouling polymer brushes on the wafer scale

Angus Hucknall, Andrew J. Simnick, Ryan T. Hill, and Ashutosh Chilkoti^{a)}

Department of Biomedical Engineering, Box 90281 and Center for Biologically Inspired Materials and Material Systems, Duke University, Durham, North Carolina 27708

Andres Garcia,^{b)} Matthew S. Johannes,^{c)} Robert L. Clark,^{d)} and Stefan Zauscher^{a)}

Department of Mechanical Engineering and Materials Science, Box 9030, and Center for Biologically Inspired Materials and Material Systems, Duke University, Durham, North Carolina 27708

Buddy D. Ratner

Department of Bioengineering and Chemical Engineering, UWEB, University of Washington, Seattle, Washington 98195

(Received 24 April 2009; accepted 15 May 2009; published 10 June 2009)

In this article, the authors describe new approaches to synthesize and pattern surfaces with poly[oligo(ethylene glycol) methyl methacrylate] (POEGMA) polymer brushes synthesized by surface-initiated atom transfer radical polymerization. These patterned coatings confer “nonfouling” properties protein and cell resistance—to the surface in a biological milieu. The versatile routes for the synthesis of POEGMA demonstrated here offer clear advantages over other techniques previously used in terms of their simplicity, reliability, and ability to pattern large-area substrates. They also demonstrate that POEGMA polymer brushes can be patterned directly by photolithography, plasma ashing, and reactive ion etching to create patterns at the micro- and nanoscale over large areas with high throughput and repeatability, while preserving the protein and cell resistance of the POEGMA brush. © 2009 American Vacuum Society. [DOI: 10.1116/1.3151968]

I. INTRODUCTION

The function of miniaturized biodevices, such as biosensors and microarrays, depends critically on a sufficiently large signal-to-noise ratio, achieved by minimizing nonspecific binding and maximizing specific binding between target biomolecules.^{1,2} Self-assembled monolayers (SAMs) containing multiple ethylene glycol units [ranging from oligo- to poly(ethylene glycol) (OEG or PEG)]^{3–5} are widely used as coatings on surfaces to prevent protein nonspecific adsorption and cell adhesion. Although these SAMs are easily prepared at sufficiently high surface densities, they often lack uniformity and robustness and are typically confined to oxide or metal surfaces where they offer a limited number of architectures and chemistries. To address these issues, Chilkoti and co-workers^{6–8} were the first to synthesize nonfouling PEG-functionalized polymer brushes via surface-initiated atom transfer radical polymerization (SI-ATRP). These poly[oligo(ethylene glycol) methyl methacrylate] (POEGMA) brushes consist of a methacrylate polymer backbone with OEG side chains that endow the polymer brush with protein and cell-resistant “nonfouling” properties.⁸ The

thickness of the POEGMA brush can be finely tuned by varying the initiator surface graft density and the polymerization conditions.⁷

As we survey the field of protein and cell-resistant surfaces, especially within the context of polymer coatings synthesized by surface-initiated polymerization, two challenges obviously remain: (1) expanding the range of materials that are capable of supporting the formation of POEGMA (and other polymers) brushes via simple and widely useful methods and (2) creating a set of complementary approaches to pattern these polymer brushes with high fidelity and reliability on a wafer scale for device production without compromising their nonfouling properties. To date, the range of substrates that have been modified with POEGMA brushes is largely limited to gold, silicon, and metal oxide surfaces that readily support the formation of SAMs capable of presenting an ATRP initiator. Unfortunately, however, many technologically useful materials, such as plastics, do not support the formation of SAMs and only recently have there been several reports of SI-ATRP of PEG monomers from halogenated polymer surfaces, most for purposes of control of fouling.^{9–14} Furthermore, we and others demonstrated methods for the patterning of POEGMA (Ref. 8) and other polymer brushes^{15–19} by soft lithography, dip-pen nanolithography (DPN), and e-beam lithography.²⁰ A significant need still exists to reliably pattern nonfouling polymer brushes at the *wafer scale* with high precision, fidelity, and with features that span a large range of sizes, ranging from hundreds of nanometers to hundreds of micrometers, for application in

^{a)}Authors to whom correspondence should be addressed; electronic mail: chilkoti@duke.edu; zauscher@duke.edu

^{b)}Present address: Liquidia Technologies, Inc., Research Triangle Park, NC 27709.

^{c)}Present address: Applied Physics Laboratory, Laurel, MD 20723.

^{d)}Present address: School of Engineering and Applied Sciences, University of Rochester, Rochester, NY 14627.

bioanalytical devices. This article addresses both these related challenges.

First, we present two simple methods to grow protein- and cell-resistant POEGMA brushes on the surface of a broad range of materials. In these methods, ATRP initiator layers are deposited by two complementary approaches: (1) spin or dip coating a macroinitiator of poly(vinylbenzyl chloride) (PVBC) and (2) plasma polymerization of 2-chloroethylmethacrylate (2-CEMA). Previously, Teare *et al.*²¹ demonstrated a method for growing polymer brushes by SI-ATRP from initiator layers formed by pulsed plasma-chemical deposition of 4-vinylbenzyl chloride or 2-bromoethylacrylate. PVBC has also been used as a macroinitiator for ATRP.^{22,23} Furthermore, Farhan and Huck demonstrated the growth of poly(*N*-isopropyl acrylamide) from a variety of plasma oxidized polymeric films. Plasma oxidation was used to create surface hydroxyl groups, which were then functionalized with a trichlorosilane-terminated ATRP initiator.²⁴ Although these methods have been used previously to form ATRP initiator layers, we are not aware of any studies that harnessed these methods for the deposition of a polymerization initiator on a broad range of substrates to enable the synthesis of protein- and cell-resistant coatings.

Second, we demonstrate a set of robust and reliable methods to pattern POEGMA brushes (and potentially other polymer brushes) with high precision and fidelity at the wafer scale for technological application of these polymer brushes in bioanalytical devices and for fundamental studies of cell-surface interactions. Although we have previously demonstrated micro- and nanopatterning of POEGMA brushes by microcontact printing and DPN, respectively,⁸ these methods are not viable for large-area patterning for commercial applications. Here we show that photolithography, combined with reactive ion etching (RIE) or plasma ashing, provides a rapid and convenient method to directly pattern POEGMA brushes on the micro- and nanoscale and over large areas.

Photolithography generally involves the exposure and subsequent selective removal of a polymeric photoresist.^{25–27} A photoresist covered substrate surface is selectively patterned by exposing the resist through a mask using UV light.²⁸ Spatial resolution is largely determined by the Abbe diffraction limit²⁹ (a far-field effect), which limits the feature size to about half of the wavelength of the light used. The use of deep UV radiation and other technological advancements has afforded features of less than 200 nm.²⁷ Although Prucker and Ruhe³⁰ realized the potential of photolithography to microstructure molecularly thin polymer layers directly a decade ago, this methodology has surprisingly found little use for patterning of polymer brushes.³¹ More commonly, photolithography is used to pattern a substrate such that the initiator can be selectively attached to the patterned regions.³² Prucker *et al.*³³ used “soft” UV to activate a surface-bound azobisisobutyronitrile initiator selectively in a phototemplating approach. In an effort to increase patterning resolution, interference lithography has been used to create nanoscale patterns of polystyrene brushes over a large surface area.³⁴

In this article, we explore the fabrication of POEGMA polymer brushes through novel, robust, and easy synthesis methods using spin coated, dip coated, or plasma polymerized initiator layers and patterning of these POEGMA brushes directly via photolithography, RIE, and plasma ashing at the micro- and nanoscale. To our knowledge, this is the first time that these methods have been used to pattern non-fouling polymer brushes over large areas.

II. METHODS AND MATERIALS

A. Synthesis of POEGMA brushes on silicon wafers

The initiator, [11-(2-bromo-2-methyl)propionyloxy]undecyl trichlorosilane, was used as received from Rich Medicine (Hong Kong, China). All other chemicals were used as received from Sigma-Aldrich Corporation (St. Louis, MO). Conductive, doped silicon wafers (*p*-type, <111>-oriented, 0.1 Ω cm resistivity) were purchased from Virginia Semiconductors (VA). SI-ATRP of OEGMA was carried out as reported previously.^{6,7} Briefly, cleaned silicon wafers and glass slides were immersed into a 0.05% (weight/volume) solution of [11-(2-bromo-2-methyl)propionyloxy]undecyl trichlorosilane in anhydrous toluene, and silanization was allowed to proceed for 10 min. The silanized wafers were then removed from the silane solution, rinsed with tetrahydrofuran (THF) and hot water (80 °C), and dried under a stream of N₂ gas. The initiator coated wafers were then immersed in a polymerization solution of CuBr (143 mg, 1.0 mmol), bipyridine (312 mg, 2.0 mmol), de-ionized (DI) water (degassed, 3 ml), methanol (12 ml), and OEGMA (8 g, 16.7 mmol). After a specified time under nitrogen purge, the samples were removed from the solution to stop the polymerization, rinsed with methanol, and finally dried under a stream of N₂ gas. POEGMA coatings with thicknesses of 35, 60, and 100 nm were synthesized by this procedure by varying the polymerization time from 2 to 24 h. The dry film thicknesses were measured with an M-88 spectroscopic ellipsometer (J. A. Woollam Co., Inc.) at angles of 65°, 70°, and 75° and wavelengths from 400 to 800 nm. A Cauchy layer model was used to determine film thickness using the software package provided by Woollam Co.

B. Synthesis of POEGMA brushes on a range of substrates

Following Dressick *et al.*,³⁵ Si wafers were first vapor treated for 10 min with a 10% (v/v) solution of hexamethyldisilazane in acetone in a closed container to promote the adhesion of the spin-coated PVBC initiator layers. A solution of 1% (w/v) PVBC in toluene was prepared and filtered through a 0.2 μ m pore Teflon filter immediately prior to spin coating at 3000 rpm for 30 s. The coated wafers were baked in a vented oven at 90 °C for 30 min to remove excess toluene from the PVBC film. Poly(styrene) (PS), poly(methyl methacrylate) (PMMA), poly(ethylene terephthalate) (PET), and poly(ethylene) (PE) samples used in the preparation of dip-coated PVBC initiator layers were first cleaned with isopropyl alcohol to remove organic surface contami-

nants. The substrates were then dipped into a solution of 10% (w/v) PVBC in toluene for 1 s and allowed to dry. Dip coating was repeated twice and the samples were then placed in a vacuum oven at 50 °C for 30 min to remove excess toluene from the PVBC film.

Glass cover slips (15 mm, Ted Pella), used for the deposition of plasma polymerized initiator layers, were first etched in argon for 5 min at 40 W. The cover slips were then coated with 2-CEMA (Pfaltz and Bauer, Inc., heated to 33 °C) for 1 min at 80 W in order to form an adhesion layer, after which the power was lowered to 10 W for 5 min and finally to 5 W for 5 min. A pressure of 250 mTorr was maintained throughout the entire process.

To grow POEGMA brushes on the dip-coated, spin-coated, and plasma polymerized surfaces, substrates were immersed in a ATRP polymerization solution of CuBr (143 mg, 1.0 mmol), bipyridine (312 mg, 2.0 mmol), de-ionized water (degassed, 3 ml), methanol (12 ml), and OEGMA (8 g, 16.7 mmol).^{6–8} After a specified time under nitrogen purge, the samples were removed from the solution to stop the polymerization, then rinsed with methanol, and dried under a stream of N₂ gas.

C. Photolithography using positive photoresist

The POEGMA brush substrates were first washed and sonicated in ethanol to remove particulates from the surface. A positive photoresist (Shipley 1813) was then spin coated (Headway spinner) on the POEGMA layer at a ramp speed of 2000 rpm and a spin speed of 3200 rpm for 30 s. The samples were then placed on a hot plate for 1 min at 115 °C and subsequently exposed to UV light ($\lambda=365$ nm, 12.0 mW/cm²) for 10 s using a Süss MA6 mask aligner in hard contact mode. The photoresist was developed for various times ranging from 30 to 90 s using MF-319 (Microposit) photoresist developer at room temperature. After the development step, the samples were thoroughly rinsed with DI water and dried in a stream of N₂. The typical thickness of the patterned photoresist was 1.5 μ m, measured using a Veeco Dektak 150 profilometer. Due to the significant difference in thickness between the POEGMA layer (~35 nm) and the photoresist (~1.55 μ m), the patterned photoresist was used as a mask in the RIE or plasma ashing step to preferentially remove the thin layer of exposed POEGMA. During RIE, the samples were exposed to a plasma of active oxygen atoms in the reactive ion etcher (Trion Technology Phantom II) using 150 W at 13.56 MHz in a 200 mTorr oxygen atmosphere for 1–2 min to completely etch the exposed POEGMA regions. During plasma ashing, samples were exposed to oxygen plasma for 30–90 s in an Emitech K-1050X, operating at a frequency of 13.56 MHz and 10–80 W of rf power at a pressure of ~1.6 Torr. After RIE or plasma ashing, the photoresist on the protected regions was easily removed by immersing the substrates in a photoresist stripper (AZ-400T Photoresist Stripper) for 2 min. The samples were then rinsed with copious amounts of Milli-Q grade water and dried in a stream of N₂. The

POEGMA patterns were imaged by optical microscopy and by TappingMode atomic force microscopy (AFM) in air.

D. Photolithography using negative photoresist

The POEGMA brush substrates were first washed and sonicated in ethanol to remove particulates from the surface. A negative photoresist (Futurrex NR9–1500PY) was then spin coated (Headway spinner) onto the POEGMA layer at a ramp speed of 3000 rpm and a spin speed of 4000 rpm for 30 s. The samples were then placed on a hot plate for 2 min at 150 °C. Samples were exposed to UV light ($\lambda=365$ nm, 12.0 mW/cm²) for 11 s using the Süss MA6 mask aligner in hard contact mode. After exposure, the samples were baked on a hot plate at 100 °C for 60 s. The photoresist was then developed for various times ranging from 5 to 20 s using (Futurrex RD6) photoresist developer at room temperature. The samples were thoroughly rinsed with DI water and dried in a stream of N₂. The thickness of the patterned photoresist was measured using with a profilometer (Veeco Dektak 150) and was found to be 1.1 μ m. Due to the significant difference in thickness between the POEGMA layer (~35 nm) and the photoresist (~1.1 μ m), the patterned photoresist was used as a mask in the RIE or plasma ashing step to preferentially remove the thin regions of exposed POEGMA. During RIE, the samples were exposed to a plasma of active oxygen atoms in a reactive ion etcher (Trion Technology Phantom II) using 150 W at 13.56 MHz in a 200 mTorr oxygen atmosphere for 1–2 min to completely etch the exposed POEGMA regions. During plasma ashing, samples were exposed to oxygen plasma for 30–90 s in an Emitech K-1050X operating at a frequency of 13.56 MHz and 10–80 W of rf power at a pressure of ~1.6 Torr. After RIE or plasma ashing, the photoresist on the protected regions was easily washed away by 5 min sonication in a bath of photoresist stripper (AZ Futurrex RR5). The samples were then rinsed with isopropanol and dried in a N₂ stream. The POEGMA patterns were imaged using an optical microscope and the height of the features was obtained by TappingMode AFM imaging in air.

E. Fluorescence microscopy

To evaluate the protein resistance of the patterned POEGMA layers, samples were immersed in a 1 mg/ml solution of fluorescein isothiocyanate (FITC)-labeled bovine serum albumin (BSA) in phosphate buffered saline (PBS) for 30 min. Samples were then removed from the FITC-BSA solution, rinsed by a 10 s immersion in fresh PBS, and blown dry with nitrogen. The samples were then imaged using a Nikon Eclipse TE2000 fluorescence microscope.

F. X-ray photoelectron spectroscopy analysis

X-ray photoelectron spectroscopy (XPS) was performed on a Kratos Axis Ultra spectrometer (Shimadzu) equipped with a monochromatic Al K α source, a hemispherical analyzer, and a low energy flood gun for charge compensation of insulators. Low-resolution survey scans were obtained from

TABLE I. Observed and expected at. % obtained from survey scans and high-resolution C 1s scans shown in Fig. 1.

		C 1s					Survey		
		1	2	3	4	5	C	O	Cl
2-CEMA	Observed	46.6	23.3	11.4	10.4	8.1	79.9	14.4	5.6
	Expected	33.3	16.6	16.6	16.6	16.6	66.6	22.2	11.1
2-CEMA-POEGMA	Observed	17.5	8.7	56.1	8.7	8.7	70.3	29.6	...
	Expected	16.6	8.3	58.3	8.3	8.3	66.6	33.3	...
PVBC	Observed	64.2	21.4	14.3	91.5	0.5	7.9
	Expected	66.6	22.2	11.1	90.0	...	10.0
PVBC-POEGMA	Observed	17.2	8.6	56.9	8.6	8.6	70.5	29.0	0.5
	Expected	16.6	8.3	58.3	8.3	8.3	66.6	33.3	...

0 to 1200 eV with a 1 eV step size and 200 ms dwell time. High-resolution C 1s scans were obtained from 275 to 295 eV with a 0.1 eV step size and 200 ms dwell time. The spectra were analyzed off line with CASAXPS software (Casa Software Ltd., Version 2.2.79).

G. Cell growth and imaging

Human umbilical vein endothelial cells (HUVECs) were seeded onto both 2-CEMA and 2-CEMA-POEGMA surfaces at a density of 30 000 cells cm⁻² in serum containing media. Cell attachment was allowed to proceed for 12 h at 37 °C in 5% CO₂. Samples were stained with the cytoplasmic stain Cell-Tracker-Orange and the nuclear stain Hoechst 3342 (Invitrogen, Carlsbad, CA) and imaged immediately using a Zeiss LSM 510 inverted confocal microscope. Patterned POEGMA surfaces exposed to a HUVEC solution under the same conditions were imaged with a Nikon Eclipse TE2000 fluorescence microscope.

III. RESULTS

A. Simplified fabrication of POEGMA surfaces

In our previous studies, substrates modified with POEGMA brushes were limited to materials that support the formation of SAMs capable of presenting ATRP initiators, such as gold, silicon, and metal oxides. However, the surfaces of many technologically relevant materials, such as plastics, do not support SAM formation. To overcome this limitation, we investigated three versatile methods for deposition of an initiator layer: (1) plasma polymerization of 2-CEMA on glass, (2) dip coating a range of industrially relevant, planar polymer substrates (PS, PMMA, PET, and PE) in a solution of PVBC, and (3) spin coating of PVBC on silicon. These layers were then used to initiate SI-ATRP of OEGMA. We chose these methods because (1) they are capable of functionalizing a broad range of materials and (2) they do not rely on custom-fabricated initiators deposited as SAMs.

We used x-ray photoelectron spectroscopy to assess the functionalization of substrates with initiator. The survey scans, summarized in Table I, provide information on the overall surface chemical composition. We found that in all cases, the overall chemical composition matched the expected composition reasonably well. High-resolution C 1s

spectra (Fig. 1) provide insight into the chemical bonding environment of carbon. In Table I, we compare the observed contributions of each chemical state of carbon to the expected contributions based on the stoichiometric ratios present in each chemical structure. In the case of plasma polymerized 2-CEMA, the observed contributions of oxygen and chlorine are less than expected. This is a result of the higher susceptibility of C–Cl and C–O bonds to degradation during plasma exposure.³⁶ The high-resolution C 1s peak of the poly(OEGMA) brushes can be fitted with five unique carbon moieties: CH_x (285.0 and 285.7 eV), C–O–R (286.6 and 287.3 eV), and COOR (289.1 eV).³⁷ From the deconvoluted C 1s spectra of the poly(OEGMA) brush seen in Figs. 1(b) and 1(d), the sum of components 3 and 4 arising from the pendant oligo(ethylene glycol) side chains accounts for 64.8% and 65.5% of the total signal, respectively, which is

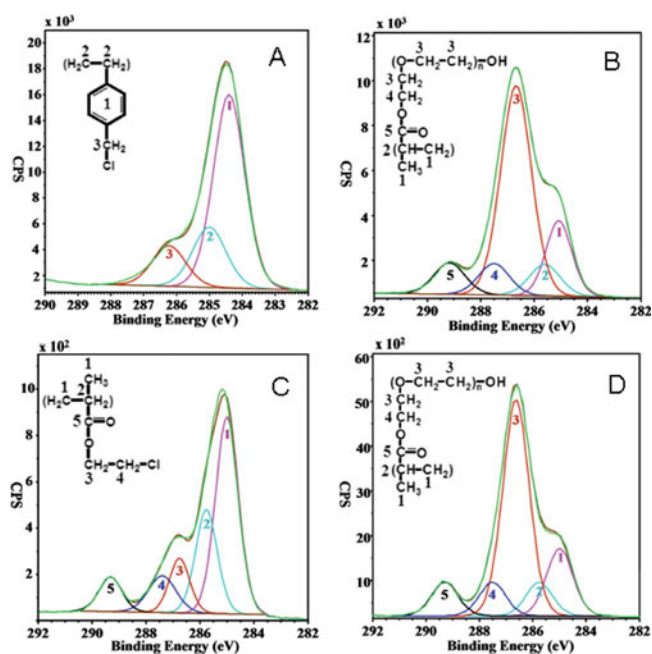


FIG. 1. (Color online) High-resolution spectra of the C 1s peak (green envelope) and corresponding chemical structure (inset) of substrates [(a) and (c)] before and [(b) and (d)] after OEGMA polymerization on initiator functionalized substrates. Fitted peaks are numbered to correspond to labeled carbons within each chemical structure. Polystyrene dip coated with PVBC (a) before and (b) after SI-ATRP of OEGMA. Plasma-polymerized 2-CEMA (c) before and (d) after SI-ATRP of OEGMA.

TABLE II. Observed at. % obtained from XPS spectra taken before and after fetal bovine serum (FBS) incubation.

		Observed at. %			
		N	C	O	Cl
2-CEMA	Before	0	80.0	14.4	5.7
	After	3.20	75.1	16.1	5.6
2-CEMA-POEGMA	Before	0	70.3	29.7	0
	After	0	70.3	29.7	0

within the experimental error. The ratios of the carbon moieties, obtained by deconvolution of the high-resolution C 1s spectra of POEGMA brushes synthesized by the three different methods, revealed no significant differences and were close to those obtained previously for POEGMA.^{6,7} These results suggest that our initiator deposition methods are robust and apparently lead to chemically well defined POEGMA brush structures on the variety of substrates tested.

The resistance to nonspecific protein adsorption of the POEGMA brush layers grown on plasma-deposited initiator layers was evaluated by first incubating the 2-CEMA and 2-CEMA-POEGMA surfaces in undiluted fetal bovine serum for 12 h and then subjecting the substrates to XPS analysis. The XPS data in Table II show that there is considerable protein adsorption on the 2-CEMA surface ($N=3.2$ at. %) but no detectable protein adsorption on the POEGMA modified substrates. Furthermore, the resistance to nonspecific protein adsorption of the POEGMA brush layers grown on plasma-deposited initiator layers was evaluated by first incubating the 2-CEMA and 2-CEMA-POEGMA surfaces for 12 h in a solution of human umbilical vein endothelial cells in serum containing media, with subsequent fluorescence imaging of the surface. Figure 2 shows that the POEGMA brushes resisted cell attachment, as no fluorescence could be observed. These results further support the conclusion that these surfaces are protein resistant, as anchorage dependent cells are extraordinarily sensitive to trace levels of adsorption of extracellular matrix proteins such as fibronectin, which can provide anchorage sites for cells via the formation of

focal contacts at levels corresponding to arginine-glycine-aspartic acid (RGD) surface concentrations of as low as 10 fmol/cm^2 .^{38,39}

B. Photolithographic patterning of POEGMA brush surfaces

Although photolithography is an established, cost-effective, and high-throughput technique capable of patterning large surface areas with micrometer and submicrometer features, surprisingly little work has been reported on its use for patterning polymer brushes. Here we used photolithography to directly pattern POEGMA brush surfaces. Both positive and negative tone photoresists were used to fabricate a variety of patterns with feature sizes ranging from 300 nm to $200 \mu\text{m}$ on 35-nm-thick POEGMA brushes, synthesized on SiO_2 and glass substrates. The stepwise approach for pattern formation is schematically shown in Fig. 3.

Photoresists tend to be sensitive to processing conditions and yield poor pattern transfer if conditions are not optimized. Since the presence of POEGMA polymer brushes on SiO_2 substrates confers wettability and adhesion properties to the substrate surface that are incompatible with standard photolithographic recipes, optimal exposure and etch conditions had to be determined after rigorous and iterative experimentation (see Methods and Materials section for details). However, once a set of patterning conditions was determined, patterning of the POEGMA thin films was accomplished quickly with high throughput, spatial resolution, and fidelity. Figure 4 shows optical images of a range of patterned POEGMA samples obtained after plasma ashing and photoresist stripping. The darker regions indicate the presence of POEGMA and the lighter regions the SiO_2 background. These images exemplify the wide variety of geometries and dimensions that can be achieved using photolithography.

To assess potential changes or damage to the brush surface due to the patterning process, we imaged the POEGMA coated substrates before and after patterning with AFM TappingMode in air, a typical result is shown in Fig. 5. Figure 5(c) shows that the feature has a uniform height of $\sim 35 \text{ nm}$, in agreement with the ellipsometric measurements of the unpatterned POEGMA layer prior to patterning. Furthermore, the root-mean-squared (rms) roughness of 0.9 nm for a $30 \times 30 \mu\text{m}^2$ feature before and after patterning suggests that

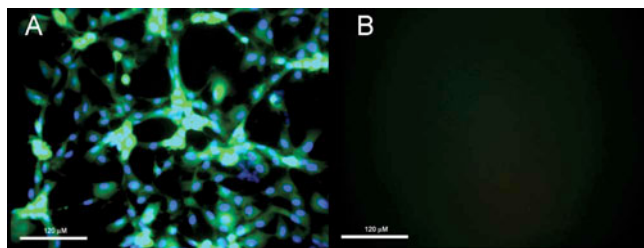


FIG. 2. (Color online) Fluorescence images ($20\times$) of (a) 2-CEMA and (b) 2-CEMA-POEGMA after exposure to HUVECs for 24 h and subsequent cell staining. The POEGMA coating eliminated cell adhesion. Scale bars represent $120 \mu\text{m}$.

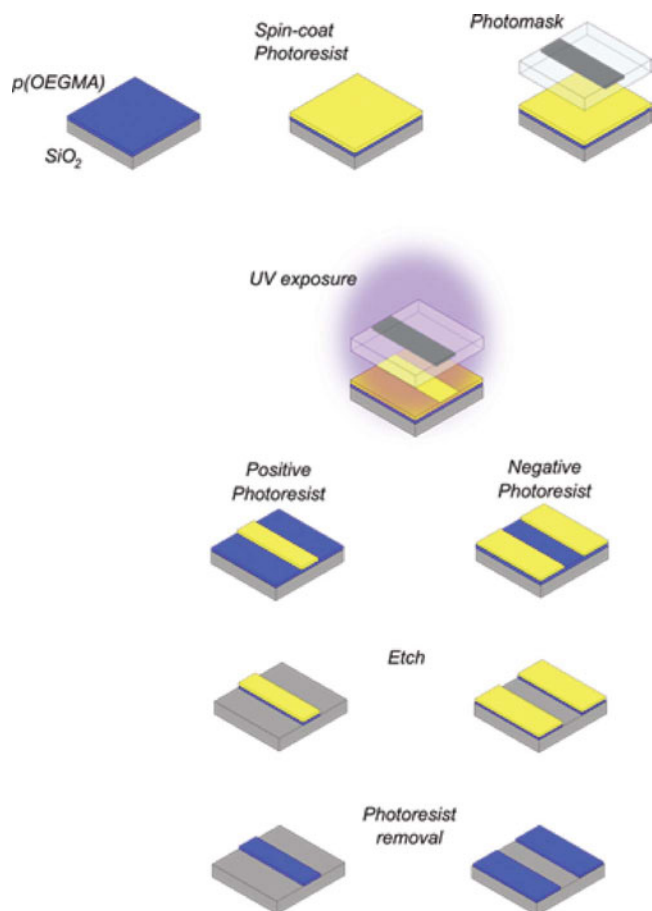


FIG. 3. (Color online) Schematic representation of POEGMA patterning via photolithography using both positive and negative photoresists.

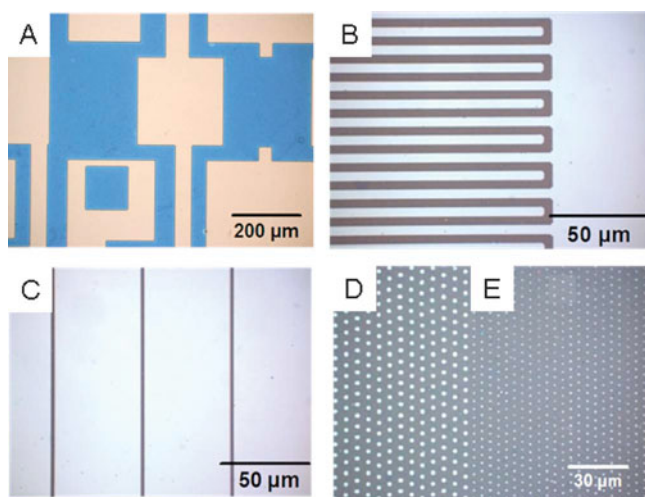


FIG. 4. (Color online) (a) Optical image (20 \times) of patterned POEGMA on SiO_2 . (b) Optical image (100 \times) of 5- μm -wide POEGMA lines. (c) Optical image (100 \times) of 3- μm -wide poly(OEGMA) lines on a SiO_2 background. [(d) and (e)] Optical image (100 \times) of patterned POEGMA sample showing circular SiO_2 features with diameters of (d) 2 μm and (e) 0.5 μm . The dry brush height was ~ 35 nm in all cases.

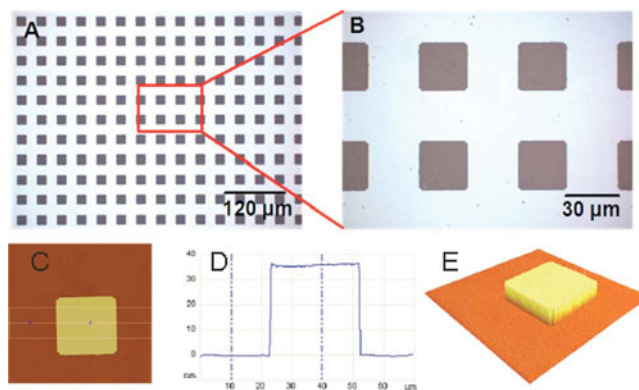


FIG. 5. (Color online) [(a) and (b)] Optical images of $30 \times 30 \mu\text{m}^2$ POEGMA squares on SiO_2 background at (a) 20 \times and (b) 100 \times . (c) Topographical AFM image of $30 \times 30 \mu\text{m}^2$ POEGMA square on SiO_2 with its corresponding height profile (d), and rendered 3D image (e) showing a uniform feature height of 35 nm.

no significant changes in surface topography occurred. Figures 5(c)–5(e) also show that the etching was highly unidirectional and perpendicular to the SiO_2 substrate, yielding vertical walls with sharp edges. These observations suggest that no significant changes in the surface morphology of the POEGMA layer are introduced during the various photolithographic steps and suggest that no topographically measurable remnants of photoresist remain.

The photoresist development time is a critical variable to achieve high-fidelity patterns. For example, for positive tone photoresist, developing times in excess of 70 s led to undes-

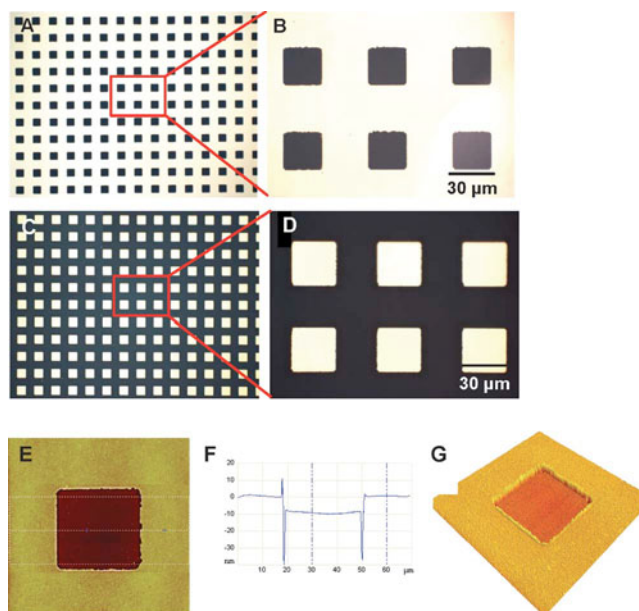


FIG. 6. (Color online) [(a) and (b)] Optical images of $30 \times 30 \mu\text{m}^2$ POEGMA squares on a Au-backfilled background at (a) 20 \times and (b) 100 \times . [(c) and (d)] Optical images of $30 \times 30 \mu\text{m}^2$ Au squares on a POEGMA background at (c) 20 \times and (d) 100 \times . (e) Topographical AFM image of a $30 \times 30 \mu\text{m}^2$ Au square in POEGMA background, with its corresponding height profile (f), and rendered 3D image (g) showing a height step difference of ~ 10 nm between the 25-nm-thick Au and the 35-nm-thick POEGMA brush layer.

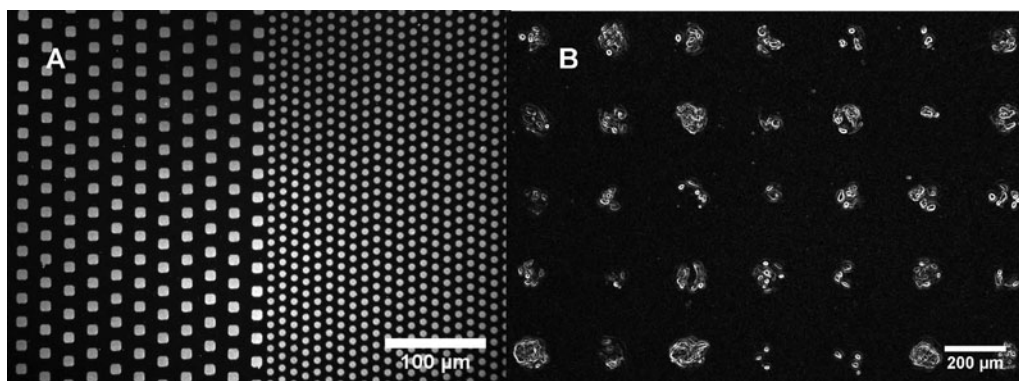


FIG. 7. (a) Fluorescence image ($20\times$) of $10\ \mu\text{m}$ SiO_2 square features and $5\ \mu\text{m}$ SiO_2 circular features on a POEGMA background after a 30 min exposure to a 1 mg/ml solution of FITC-labeled BSA. Scale bar represents $100\ \mu\text{m}$. (b) Optical image ($4\times$) of $100\ \mu\text{m}$ SiO_2 circular features on a POEGMA background after 30 min exposure to a solution of 1 mg/ml fibronectin in PBS and after a 12 h incubation with human umbilical vein endothelial cells. The dry brush height was $\sim 35\ \text{nm}$ in all cases.

ired overdevelopment, where both unexposed and exposed photoresists were removed. For positive and negative photoresists, development times of about 50 and only 8 s, respectively, were found to be optimal. Similarly, the rf power settings and exposure times are important variables for successful brush patterning. For example, low rf power settings or short exposure times cause incomplete POEGMA brush removal. For ashing a 30–100-nm-thick POEGMA layer, we found that 75 W rf power applied for a period of 90 s provided good processing conditions to remove the brush layer. The relatively high rf power setting ensured the complete removal of the POEGMA layer while minimizing horizontal etch into the polymer layer, thus ensuring high-fidelity features.

POEGMA patterns were also created via metal “lift-off” lithography (Fig. 6). Figures 6(a) and 6(b) show optical images of $30\times 30\ \mu\text{m}^2$ POEGMA squares (darker) on a gold background (lighter), and Figs. 6(c) and 6(d) show optical images of $30\times 30\ \mu\text{m}^2$ Au squares (lighter) on a POEGMA background (darker) after gold deposition and removal of the positive photoresist. Figures 6(e)–6(g) show the Tapping-Mode AFM height image of one of the $30\times 30\ \mu\text{m}^2$ Au squares from Fig. 6(c), the corresponding cross-sectional profile, and a three-dimensional (3D) image of the feature, respectively. The cross-sectional profile confirms the expected height difference of $\sim 10\ \text{nm}$ between the 25-nm-thick Cr/Au film in the squares and the $\sim 35\text{-nm}$ -thick POEGMA background. This proof-of-concept experiment demonstrates the ability to introduce a new material into the patterned POEGMA brush. For example, the gold patches may be used as a substrate for the self-assembly of suitably functionalized alkanethiols that may serve as initiators for the synthesis of a variety of polymer brushes, or as linkers for bioconjugation of proteins. Thus, patterned POEGMA brush substrates with potential applications for biosensing, for use in protein and cell arrays, and in microfluidic devices can be easily fabricated.

C. Protein and cell resistance of patterned POEGMA

Patterned POEGMA surfaces on SiO_2 were exposed to solutions of proteins and cell containing media to evaluate the protein and cell adhesion resistance of the patterned brush surfaces. Figure 7 shows that proteins and cells deposited only on the areas not functionalized with POEGMA brushes. These results suggest that the protein [Fig. 7(a)] and cell resistance [Fig. 7(b)] of the POEGMA coating is retained throughout the patterning process, and that the resulting patterns can be used as a template for producing protein and cell patterns.

IV. CONCLUSIONS

The ability to selectively control protein and cell adhesion over large surface areas is a fundamental requirement for any functional surface that contacts biological fluids. While achieving control of these phenomena is a challenging and complex problem, the application of nonfouling surfaces such as POEGMA has proven to be a useful method for tailoring the biointerface. In this work, we have presented simplified routes for the synthesis of POEGMA brushes on a wide range of substrates and have demonstrated the use of standard and highly accessible photolithographic techniques to pattern these POEGMA coatings without compromising their protein and cell resistance. We believe that the methods described in this work have the potential to extend the use of nonfouling POEGMA coatings to a broad range of commercially interesting applications in the biomedical device, diagnostics, and cell and tissue engineering arenas.

ACKNOWLEDGMENTS

The authors thank Winston Ciridon at the NESAC/BIO Center at the University of Washington for preparation of the plasma polymerized 2-CEMA samples. This research was supported by a grant to A.C. from the Wallace H. Coulter Foundation and by NSF NIRT Grant No. 0609265 to A.C., S.Z., and R.L.C. from the National Science Foundation. The

two authors (A.H. and A.G.) contributed equally to this work.

- ¹A. Hucknall, D. H. Kim, S. Rangarajan, R. T. Hill, W. M. Reichert, and A. Chilkoti, *Adv. Mater. (Weinheim, Ger.)* **21**, 1968 (2009).
- ²A. Hucknall, S. Rangarajan, and A. Chilkoti, *Adv. Mater. (Weinheim, Ger.)* (to be published).
- ³P. Harder, M. Grunze, R. Dahint, G. M. Whitesides, and P. E. Laibinis, *J. Phys. Chem. B* **102**, 426 (1998).
- ⁴R. L. C. Wang, H. J. Kreuzer, and M. Grunze, *J. Phys. Chem. B* **101**, 9767 (1997).
- ⁵K. L. Prime and G. M. Whitesides, *J. Am. Chem. Soc.* **115**, 10714 (1993).
- ⁶H. W. Ma, D. J. Li, X. Sheng, B. Zhao, and A. Chilkoti, *Langmuir* **22**, 3751 (2006).
- ⁷H. W. Ma, M. Wells, T. P. Beebe, and A. Chilkoti, *Adv. Funct. Mater.* **16**, 640 (2006).
- ⁸H. W. Ma, J. H. Hyun, P. Stiller, and A. Chilkoti, *Adv. Mater. (Weinheim, Ger.)* **16**, 338 (2004).
- ⁹L. Li, G. P. Yan, J. Y. Wu, X. H. Yu, and Q. Z. Guo, *J. Macromol. Sci., Pure Appl. Chem.* **45**, 828 (2008).
- ¹⁰X. F. Sun, J. K. Liu, and M. L. Lee, *Anal. Chem.* **80**, 856 (2008).
- ¹¹F. Yao, G. D. Fu, J. P. Zhao, E. T. Kang, and K. G. Neoh, *J. Membr. Sci.* **319**, 149 (2008).
- ¹²J. N. Kizhakkedathu, J. Janzen, Y. Le, R. K. Kainthan, and D. E. Brooks, *Langmuir* **25**, 3794 (2009).
- ¹³L. Li, G. P. Yan, and J. Y. Wu, *J. Appl. Polym. Sci.* **111**, 1942 (2009).
- ¹⁴B. Yameen, M. Alvarez, O. Azzaroni, U. Jonas, and W. Knoll, *Langmuir* **25**, 6214 (2009).
- ¹⁵D. C. Chow, W. K. Lee, S. Zauscher, and A. Chilkoti, *J. Am. Chem. Soc.* **127**, 14122 (2005).
- ¹⁶S. J. Ahn, M. Kaholek, W. K. Lee, B. LaMattina, T. H. LaBean, and S. Zauscher, *Adv. Mater. (Weinheim, Ger.)* **16**, 2141 (2004).
- ¹⁷M. Kaholek, W. K. Lee, S. J. Ahn, H. W. Ma, K. C. Caster, B. LaMattina, and S. Zauscher, *Chem. Mater.* **16**, 3688 (2004).
- ¹⁸M. Kaholek, W. K. Lee, J. X. Feng, B. LaMattina, D. J. Dyer, and S. Zauscher, *Chem. Mater.* **18**, 3660 (2006).
- ¹⁹M. Kaholek, W. K. Lee, B. LaMattina, K. C. Caster, and S. Zauscher, *Nano Lett.* **4**, 373 (2004).
- ²⁰R. Ducker, A. Garcia, J. M. Zhang, T. Chen, and S. Zauscher, *Soft Matter* **4**, 1774 (2008).
- ²¹D. O. H. Teare, D. C. Barwick, W. C. E. Schofield, R. P. Garrod, L. J. Ward, and J. P. S. Badyal, *Langmuir* **21**, 11425 (2005).
- ²²S. Holmberg, P. Holmlund, C.-E. Wilén, T. Kallio, G. Sundholm, and F. Sundholm, *J. Polym. Sci., A: Polym. Chem.* **40**, 591 (2002).
- ²³Z. P. Cheng, X. L. Zhu, G. D. Fu, E. T. Kang, and K. G. Neoh, *Macromolecules* **38**, 7187 (2005).
- ²⁴T. Farhan and W. T. S. Huck, *Eur. Polym. J.* **40**, 1599 (2004).
- ²⁵M. Lundstrom, *Science* **299**, 210 (2003).
- ²⁶T. Ito and S. Okazaki, *Nature (London)* **406**, 1027 (2000).
- ²⁷M. Totzeck, W. Ulrich, A. Gohnermeier, and W. Kaiser, *Nat. Photonics* **1**, 629 (2007).
- ²⁸G. Tovar, S. Paul, W. Knoll, O. Prucker, and J. Ruhe, *Supramol. Sci.* **2**, 89 (1995).
- ²⁹R. C. Dunn, *Chem. Rev. (Washington, D.C.)* **99**, 2891 (1999).
- ³⁰O. Prucker and J. Ruhe, *Langmuir* **14**, 6893 (1998).
- ³¹M. Husemann, M. Morrison, D. Benoit, K. J. Frommer, C. M. Mate, W. D. Hinsberg, J. L. Hedrick, and C. J. Hawker, *J. Am. Chem. Soc.* **122**, 1844 (2000).
- ³²F. Zhou, L. Jiang, W. M. Liu, and Q. J. Xue, *Macromol. Rapid Commun.* **25**, 1979 (2004).
- ³³O. Prucker, J. Habicht, I. J. Park, and J. Ruhe, *Mater. Sci. Eng., C* **8-9**, 291 (1999).
- ³⁴C. Padeste, H. H. Solak, H. P. Brack, M. Slaski, S. A. Gursel, and G. G. Scherer, *J. Vac. Sci. Technol. B* **22**, 3191 (2004).
- ³⁵W. J. Dressick, C. S. Dulcey, S. L. Brandow, H. Witschi, and P. F. Neeley, *J. Vac. Sci. Technol. A* **17**, 1432 (1999).
- ³⁶T. M. W. G. N. Taylor, *Polym. Eng. Sci.* **20**, 1087 (1980).
- ³⁷*Surface Analysis of Polymers by XPS and Static SIMS*, Cambridge Solid State Science Series, edited by D. Briggs (Cambridge University Press, New York, 1998).
- ³⁸S. P. Massia and J. A. Hubbell, *J. Cell Biol.* **114**, 1089 (1991).
- ³⁹G. M. Harbers and K. E. Healy, *J. Biomed. Mater. Res. Part A* **75A**, 855 (2005).